International Journal of Nanomedicine

Dovepress
open access to scientific and medical research

Open Access Full Text Article

ORIGINAL RESEARCH

Netrin-1 Monoclonal Antibody-Functionalized Nanoparticle Loaded with Metformin Prevents the Progression of Abdominal Aortic Aneurysms

Zhiwei Zhang[1,*], Jiawei Zhuang[2,*], Daohan Sun[3,*], Qingwei Ding[1], Hui Zheng[1], Haixiang Li[1], Xiaoyu Zhang[1], Yaming Du[3], Teng Ma[1], Qingyou Meng[1]

[1]Department of Vascular Surgery, General Surgery Clinical Center, Shanghai General Hospital, Shanghai Jiao Tong University School of Medicine, Shanghai, People's Republic of China; [2]Department of Cardiovascular Surgery, The First Affiliated Hospital of Xiamen University, School of Medicine, Xiamen University, Xiamen, People's Republic of China; [3]Department of Vascular Surgery, The First Affiliated Hospital of Jinzhou Medical University, Jinzhou, People's Republic of China

*These authors contributed equally to this work

Correspondence: Qingyou Meng; Teng Ma, Email mengqy@163.com; m_aeolus@163.com

Background: Abdominal aortic aneurysms (AAAs) are a global health and economic burden. Therapeutic strategies to inhibit the progression of AAAs are currently lacking. Recently, the therapeutic effect of metformin on aneurysms has attracted considerable interest. However, the unfavorable pharmacokinetic properties of metformin limit its feasibility for AAA treatment.

Methods and Results: We constructed a metformin-loaded netrin-1-responsive AAA-targeted nanoparticle (Tgt-NP-Met) for AAA management. Evaluation of the therapeutic effect of Tgt-NP-Met was performed by in vitro and in vivo experiments. Our results showed that the binding of netrin-1 monoclonal antibodies enhanced the AAA-targeting capability of nanoparticles (NPs). Moreover, Tgt-NP-Met administration prevented AAA development and reduced the aneurysm diameter in apolipoprotein E (ApoE)-deficient ($ApoE^{-/-}$) mice that received continuous infusion of angiotensin II. Furthermore, metformin prevented AAA progression by inhibiting the transformation of vascular smooth muscle cells (VSMCs) from a contractile phenotype to a synthetic phenotype, which is mediated by macrophage infiltration and activation.

Conclusion: Our findings identify metformin as a functional suppressor for macrophage-mediated phenotypic transformation of VSMCs and Tgt-NP-Met as an efficient therapeutic strategy for AAA management.

Keywords: abdominal aortic aneurysm, nanoparticle, metformin, macrophage

Introduction

Abdominal aortic aneurysm (AAA) is a fatal disease in the elderly, and it is estimated that more than 200,000 patients worldwide die of ruptured AAA each year.[1,2] In clinical cases, when the maximum AAA diameter exceeds 55 mm, the incidence of AAA rupture increases significantly.[2] For these patients, surgical intervention, including open surgical or endovascular repair, may be the only choice for an efficient therapy. These procedures reduce the mortality rate of patients with large AAAs. However, postoperative complications, including long-term anticoagulation, infection, and spinal cord injury, reduce the quality of life of these patients.[3] In contrast, recent clinical studies have reported no benefits of surgical intervention for small AAAs (aneurysm diameter ranging from 30 mm to 50 mm).[1] In general, for these patients, regular imaging is usually performed; however, an effective treatment strategy to prevent further expansion of the aortic aneurysm needs to be established. Therefore, the development of novel pharmacotherapy is warranted to prevent or slow down AAA progression.

Metformin is the first-line and most widely prescribed clinical drug for patients with type II diabetes mellitus. It exerts anti-hyperglycemic effects by enhancing the sensitivity of local somatic cells, including adipocytes and myocytes, to insulin.[4,5] Attributed to a long and wide clinical application, numerous preclinical and clinical trials have investigated

Received: 10 December 2022
Accepted: 1 February 2023
Published: 6 February 2023

Graphical Abstract

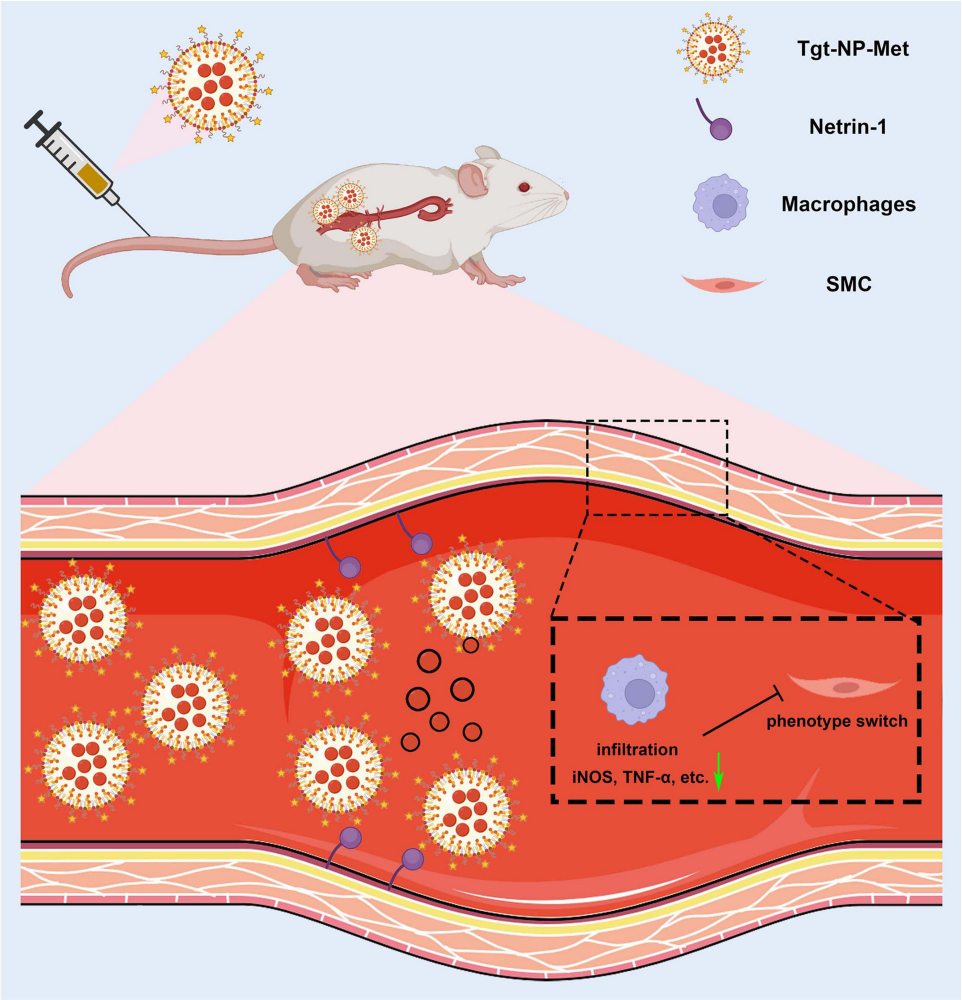

other potential therapeutic effects of this "star" drug in metabolic diseases, cardiovascular diseases, autoimmune disease, cancers, etc.[4,6] Recently, the therapeutic effect of metformin on aneurysms has attracted considerable interest. Emerging evidence suggests that metformin is associated with a lower AAA development rate and can prevent AAA progression in patients with diabetes.[7,8] However, the specific mechanism of action of metformin in the pathogenesis of AAA has not been well established. Moreover, due to unfavorable pharmacokinetic properties (half-life time ranging from 0.9 to 2.6 hours), patients often require high doses of oral metformin to maintain an effective therapy.[9] While patients could benefit from metformin, some individuals suffer from side effects, including vomiting, diarrhea, and palpitations.[10] Therefore, it is necessary to develop novel drug delivery systems to reduce drug dosage to meet therapeutic concentrations.

Advanced nanotechnology-based nanoparticles (NPs) are a promising strategy for efficient delivery of drugs or genetic materials. Polymeric NPs, such as poly(lactic acid-co-glycolic acid)-polyethylene glycol (PLGA-PEG) NPs, have been widely applied in clinical settings owing to their advantages, including good biocompatibility and biodegradability.[11] In addition, easy surface modification properties make PLGA-PEG NPs ideal candidates for targeted delivery systems, which deliver therapeutic ingredients to the desired tissues and decrease the overall toxicity at a lower drug dosage.[12] However, methods for safe and efficient delivery of drugs into the aneurysm wall have not been fully established. Many attempts have been made to develop targeting ligands, including aptamers, peptides, and monoclonal

antibodies (mAbs), for AAA.[13,14] Among these ligands, mAbs are the most widely used because of their high structural stability and specificity. A recent study has revealed that netrin-1 act at the interface of macrophage-driven injury and ECM degradation. Moreover, using single-cell RNA-sequencing (RNA-seq) of AAA, they found Netrin-1 expression peaks in human and murine aneurysmal macrophages.[15] Thus, conjugating netrin-1 mAbs to the surface may improve the targeting of PLGA-PEG NPs into AAAs.

In this study, we synthesized netrin-1 mAbs that bind PLGA-PEG NPs to enhance the therapeutic effects of metformin in AAA. The metformin release kinetics and targeting efficiency of these NPs were investigated. Moreover, the function of metformin-loaded NPs on macrophage regulation and phenotypic transformation of vascular smooth muscle cells (VSMCs) in AAA was evaluated.

Methods

Synthesis and Characterization of Metformin-Loaded Targeting NPs (Tgt-NP-Met)

Tgt-NP-Met was formulated according to a previously described procedure with modification.[16] Briefly, PLGA-PEG-MAL polymers (Mitachieve, China) and netrin-1 mAbs (Abcam, UK) or IgG mAbs (used as control; Abcam, UK) were mixed (1:1 molar ratio) in phosphate buffer solution (PBS) and then gently stirred at room temperature for 24 h. mAb-conjugated PLGA-PEG-MAL polymers were collected via centrifugation (12,000 rpm for 15 min). To form metformin-loaded NPs, metformin and mAb-conjugated PLGA-PEG-MAL polymers (1:1 w/w) were dissolved in acetone. After thorough mixing, the solution was dropped into deionized water. Acetone was then evaporated by continuous stirring at atmospheric temperature and pressure for 12 h. Finally, metformin-loaded NPs were collected via ultracentrifugation (35,000 rpm for 15 min). The morphology, particle size, and zeta potential of Tgt-NP-Met were evaluated using transmission electron microscopy (TEM; Philips, Netherlands) and dynamic light scattering (ZetaSizer Nano ZS, Malvern, UK), respectively. The release profiles of metformin from NPs were evaluated by dialysis. Briefly, 10 mg of Tgt-NP-Met was dissolved in 10 mL of normal saline and then transferred to a dialysis bag (molecular weight cutoff: 10,000–12,000 Da), which was incubated in 10 mL of PBS (pH 7.4) and vibrated on a shaker at 37°C and 80 rpm. One milliliter of the release solution was collected, and the absorbance values of these solutions were measured at 425 nm using an ultraviolet spectrophotometer (Thermo Fisher Scientific, USA) at the indicated time points (0, 12, 24, 36, 48, 72, 96, 144, and 240 h).

Cytotoxicity of Various Nanoparticles

To evaluate cytotoxicity of different NPs, VSMCs were seeded in 96-well plates at a density of 1×10^4 cells per well in 100 μL of growth medium. After 12 h, the culture medium was replaced with 100 μL of fresh medium containing gradient concentrations of NPs and incubated for 12 h. The cell viability was quantified by CCK-8 assay.

Animal Studies

All animal experiments were approved by the Institutional Animal Care and Use Committee of Shanghai Jiao Tong University and performed in accordance with the National Institutes of Health Guide for the Care and Use of Laboratory Animals.

Acute Toxicity Evaluation of Different Nanoparticles

C57BL/6 mice were randomly assigned into 3 groups: Control; Tgt-NPs and Ctrl-NPs. Equal volumes (5 mg in 200 μL of PBS) of Ctrl-NPs or Tgt-NPs were injected into mice through the tail vein. For mice in the control group, the same volume of saline was administrated. After 2 weeks, animals were euthanized. Blood samples were collected for hematological analysis (Sysmex KX-21, Sysmex Co., Japan).

AAA Induction and Nanotherapy in Mice

Apolipoprotein E (ApoE)-deficient ($ApoE^{-/-}$) mice (10–12-week-old, male; SMOC, China) were implanted with osmotic pumps containing PBS (as control) or angiotensin II (Ang II; 1 μg/min/kg; Sigma-Aldrich, USA) and allowed to develop

for 4 weeks. For in vivo localization analysis, Tgt-NPs or Ctrl-NPs containing sulfo-cyanine5 (Cy5; MedChemExpress, USA) were injected into mice through the tail vein on day 7 after osmotic pump implantation. After 24 h, the abdominal aortas were dissected and detected using the Image Visualization and Infrared Spectroscopy (IVIS) Spectrum (PerkinElmer, Inc., USA) and IF staining. For AAA therapy, equal volumes (5 mg in 200 μL of PBS) of Ctrl-NP-Met or Tgt-NP-Met were injected into mice through the tail vein on days 7, 14, and 21 after osmotic pump implantation. The systolic arterial pressure was measured using a CODA machine on day 28 (Kent Scientific, USA). The diameter of the abdominal aorta was measured, and the aorta was dissected for IF staining and enzyme-linked immunosorbent assay (ELISA) on day 28 after osmotic pump implantation.

Cell Culture and Administration

Human acute monocytic leukemia cells (THP-1) were purchased from Cell Bank of the Chinese Academy of Sciences. VSMCs were purchased from Pricella (China). For macrophage induction, THP-1 cells were cultured in RPMI 1640 supplemented with 100 nM of phorbol 12-myristate 13-acetate (Sigma-Aldrich, USA) for 72 h. VSMCs were cultured in T/G HA-VSMC medium (Pricella, China) supplemented with 10% fetal bovine serum (FBS). For co-culture, macrophages were pretreated with lipopolysaccharide (LPS, 200 nM) or LPS (200 nM) + metformin (2 mM) for 24 h. Then, the macrophages were seeded on an insert and VSMCs were seeded on the well surface to establish a co-culture system.

Macrophage Migration Assay

Macrophages (1×10^5 cells/well) were seeded on a transwell insert (Corning, USA) and cultured in RPMI 1640 medium containing 1% FBS. The transwell inserts were then placed in 24-well plates with a complete medium containing 10% FBS. The macrophages were incubated with or without metformin (2 mM) for 12 h. The cells that migrated to the lower surface of the insert were stained with a crystal violet staining solution.

IF Staining

For serial cryo-sectioning, the aorta was dissected and embedded in an optimal cutting temperature compound (Beyotime, China). IF staining was performed according to a previously described method.[15] Briefly, the tissue sections or cell samples were fixed with acetone and then blocked with 1% bovine serum in PBS for 1 h. Primary antibodies, including anti-elastin (1:500, ab217356, Abcam, UK), anti-CD68 (1:500, ab283654, Abcam, UK), anti-α-SMA (1:500, ab124964, Abcam, UK), and anti-SM22α (1:500, ab10135, Abcam, UK), were diluted in primary antibody dilution buffer and incubated with samples at 4°C overnight. The samples were then incubated with fluorescent secondary antibody at 37°C for 2 h. Images were photographed under a fluorescence inverted microscope (Lecia, Germany).

Elisa

ELISA was performed according to the manufacturer's instructions. Briefly, the AAA tissues were homogenized in 2 mL of lysis buffer and centrifuged at 12,000 rpm for 10 min. Cell supernatants from the macrophages were collected via centrifugation under the same conditions as those used for the tissues. The protein levels of iNOS, IL-6, TNF-α, IL-12A, IL-12B, α-SMA, SM22α, Myocd, and Cnn1 were determined using an ELISA kit (Sigma Biotechnology, China).

Statistical Analysis

Data are presented as mean ± SD. Comparisons between two groups were performed using a two-tailed unpaired Student's *t*-test, and those between three or more groups were performed using one-way analysis of variance (ANOVA) followed by the post-hoc Bonferroni test. Survival analysis was performed using the Log rank test. Statistical significance was set at $P < 0.05$. Statistical analyses were performed using GraphPad Prism 9.0 (GraphPad Software, USA).

Results

Development of an AAA-Targeted Metformin Delivery Nanoplatform

We designed netrin-1-responsive AAA-targeted delivery nanoparticles (Tgt-NPs) for metformin (Figure 1A). The core of these NPs contained synthesized PLGA with PEG to enhance the structural stability and hydrophilicity, which made these NPs more durable in circulation. The NPs were further functionalized with netrin-1 mAbs (IgG served as control) to gain AAA-targeting capability. The obtained NPs appeared spherical on TEM (Figure 1B), with sizes ranging from 90 nm to 1000 nm (Figure 1C). The average zeta potential of these NPs was −25.45 ± 1.66 (Ctrl-NP) and −25.45 ± 1.61 (Tgt-NP) (Figure 1D). The in vitro metformin release assay showed that approximately 80% metformin was released from the Ctrl- or Tgt-NPs after 72 h in PBS (Figure 1E).

In vitro Cytotoxicity and in vivo Safety Studies

The cytotoxicity of Ctrl-NP and Tgt-NP was detected by CCK-8 assay. Of note, both Ctrl-NP and Tgt-NP exhibited low cytotoxicity in VSMCs (Figure 2A). In vivo safety tests were performed in mice. We did not find remarkable changes in representative hematological parameters in Ctrl-NP or Tgt-NP-treated groups (Figure 2B–D). Moreover, no abnormal variations in typical biomarkers associated with hepatic and kidney functions were detected for different groups (Figure 2E–G).

Netrin-1 mAbs Modification Enhances Targeting Capability of NPs in vivo

The AAA-targeting capability of Tgt-NPs (modified with netrin-1 mAbs) and Ctrl-NPs (modified IgG mAbs) was evaluated using a mouse AAA model. Bioluminescence analysis showed that Tgt-NPs exhibited a higher relative radiant efficiency (approximately five-fold) in AAA tissues than Ctrl-NPs (Figure 3A and B). IF staining results demonstrated that more Cy5-labeled NPs accumulated in the AAA tissues, as evidenced by a stronger fluorescence intensity (Figure 3C

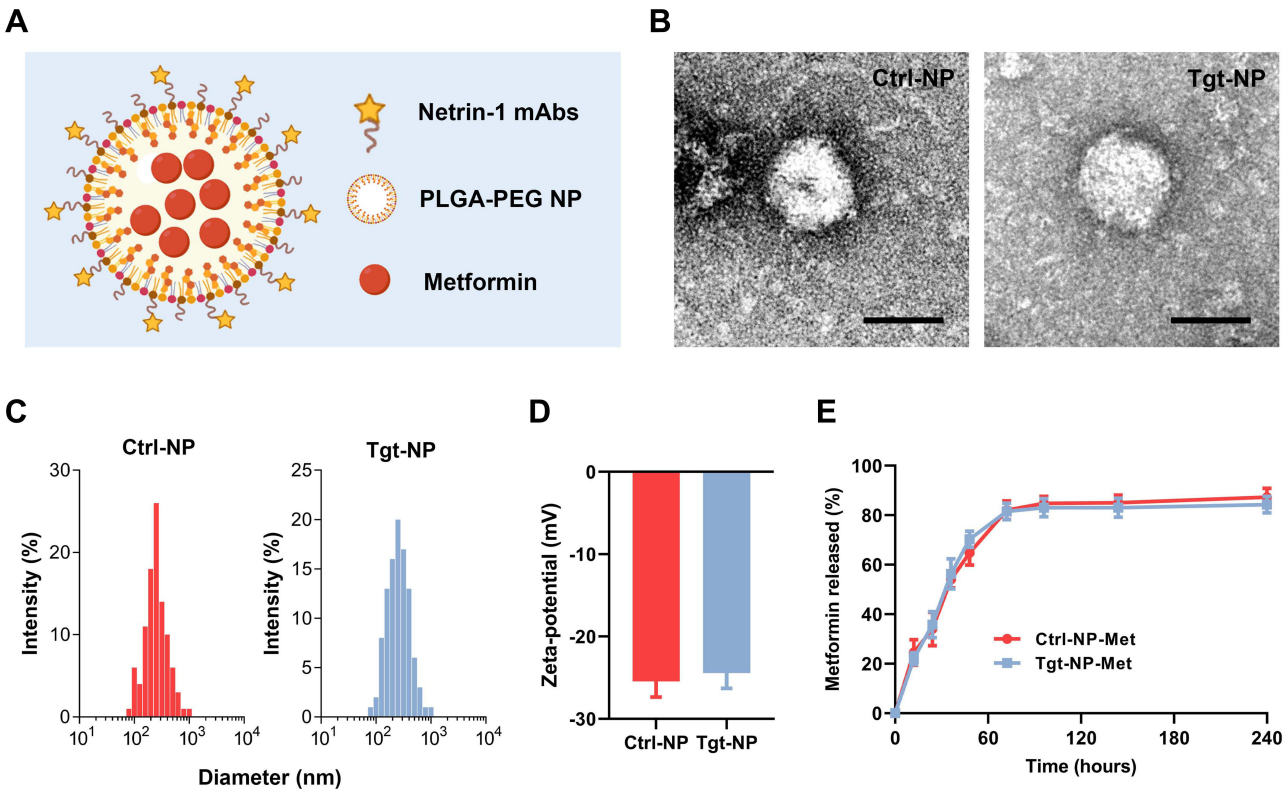

Figure 1 Synthesis and characterization of metformin-loaded netrin-1-responsive AAA-targeted NP delivery (Tgt-NP-Met). (**A**) Schematic diagram of Tgt-NP-Met synthesis. (**B**) Morphology of Ctrl- or Tgt-NP-Met observed using TEM. Scale bar = 200 nm. (**C** and **D**) Particle size (**C**) and zeta potential (**D**) of Ctrl- or Tgt-NP-Met evaluated using DLR. (**E**) Metformin release curve generated based on a dialysis release assay.

Abbreviations: AAA, abdominal aortic aneurysm; DLR, dynamic light scattering; Met, metformin; TEM, transmission electron microscopy; Tgt-NP, targeted nanoparticle.

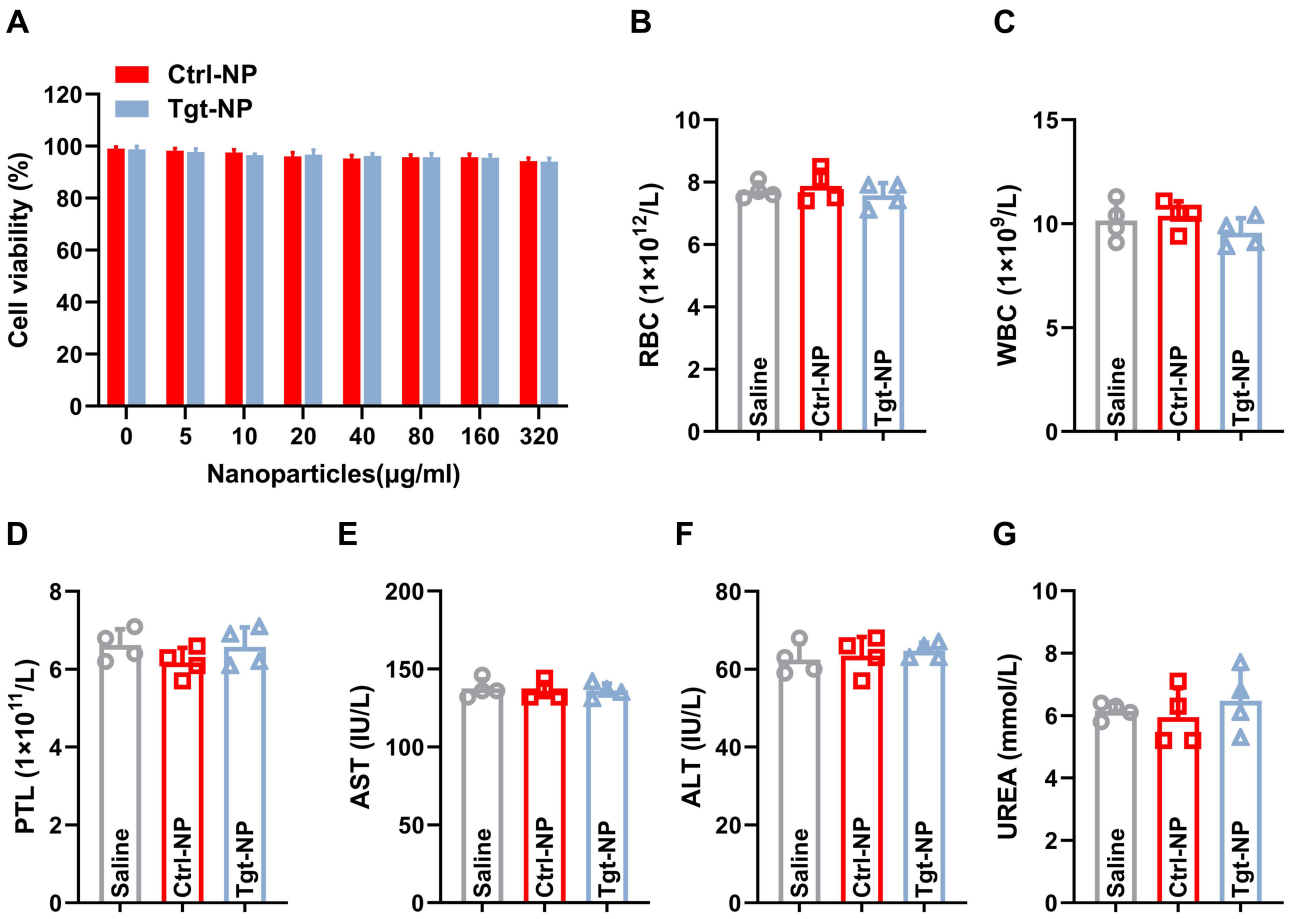

Figure 2 Cytotoxicity and in vivo toxicity evaluation of NPs. (**A**) Cell viability of VSMCs after incubation with different concentrations of Ctrl-NP or Tgt-NP for 12 h. (**B**–**D**) Whole blood count of blood samples collected from mice at day 14. (**E**–**G**) Representative biochemical markers relevant to liver and kidney functions. n = 4 per group.
Abbreviations: RBC, red blood cell; WBC, white blood cell; PLT, platelet; ALT, alanine aminotransferase; AST, aspartate aminotransferase; UREA = blood urea.

and D). These results indicate that the binding of netrin-1 mAbs enhances the AAA-targeting capability of the obtained NPs.

Tgt-NP-Met Administration Prevents AAA Progression

The therapeutic effect of Tgt-NP-Met was determined using a mouse AAA model. Systolic arterial pressure showed no differences after Ang II infusion in mice among the three groups (Figure 4A). The overall survival rate of mice on day 28 in the Tgt-NP-Met group was higher than that in the model group (Figure 4B). Tgt-NP-Met administration significantly reduced the aneurysm incidence rate (approximately 33%) compared with the model (approximately 83%) and Ctrl-NP-Met (approximately 75%) groups (Figure 4C). The maximum aneurysm diameter was calculated to evaluate the progression of aortic enlargement, which revealed markedly reduced abdominal aorta dilatation in the Tgt-NP-Met group (1.6 ± 0.41 mm) compared with the model group (2.2 ± 0.45 mm; Figure 4D and E). In addition, IF staining showed that mice in the Tgt-NP-Met group exhibited gentler elastic degradation (Figure 4F and G). These results demonstrate that Tgt-NP-Met administration prevents AAA progression in mice.

Tgt-NP-Met Administration Alleviates Macrophage-Mediated Local Inflammation and Phenotypic Transformation of VSMCs

The regulatory role of Tgt-NP-Met in macrophages was detected in an AAA mouse model. Our results demonstrated that Tgt-NP-Met treatment reduced macrophage infiltration in the AAA tissues, as evidenced by lower CD68 fluorescence

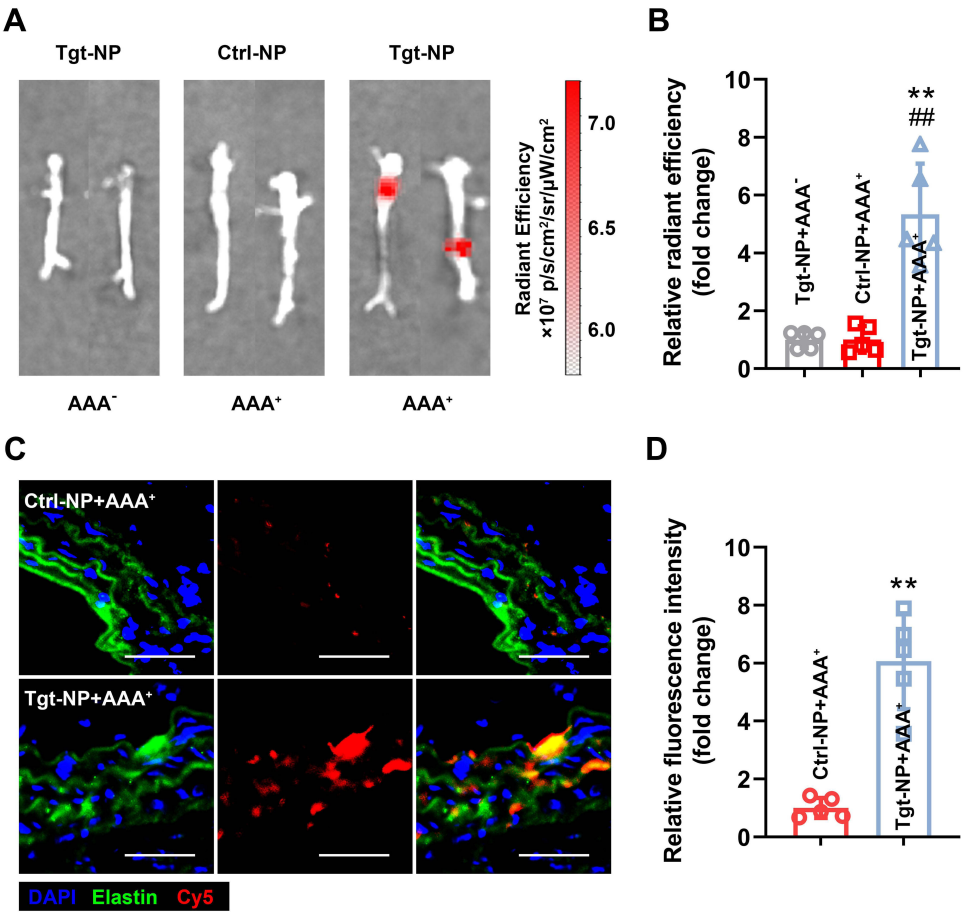

Figure 3 In vivo targeting analysis of netrin-1 mAbs binding NPs. (**A**) Tgt-NPs (Cy5-labeled, red) in vivo location detected using IVIS. (**B**) Quantification of the Cy5 fluorescence intensity. (**C**) Cy5-labeled NPs located in the abdominal aorta (indicated by elastin; green) detected using IF staining. Scale bar = 50 μm. (**D**) Quantification of the Cy5 fluorescence intensity. n = 5 per group. Significance was evaluated using one-way ANOVA with the post-hoc Bonferroni test (**B**) and Student's *t*-test (**D**). $^{**}P < 0.01$. vs Tgt-NP-Met + AAA^{-}; $^{\#\#}P < 0.01$. vs Ctrl-NP-Met + AAA^{+}.

Abbreviations: AAA, abdominal aortic aneurysm; ANOVA, analysis of variance; Cy5, cyanine5; IF, immunofluorescence; IVIS, Image Visualization and Infrared Spectroscopy; Met, metformin; Tgt-NP, targeted nanoparticle.

intensity (Figure 5A and B). ELISA assay revealed that the M1 polarization pro-inflammatory factors, including iNOS, IL-6, TNF-α, IL-12A, and IL-12B, in the AAA tissues were dramatically lower in the Tgt-NP-Met group than in the model and Ctrl-NP-Met groups (Figure 5C–G). To investigate the phenotypic transformation of VSMCs, we performed IF staining to evaluate α-SMA and SM22α in the AAA tissues of mice on day 28 post-AAA induction. Compared with the model and Ctrl-NP-Met groups, the Tgt-NP-Met group showed increased fluorescence intensity of α-SMA and SM22α, providing evidence for the inhibition of phenotypic transformation of VSMCs by Tgt-NP-Met (Figure 6A–C). These results indicate that Tgt-NP -Met treatment alleviates macrophage activation and the phenotypic transformation of VSMCs in AAA.

Metformin Reduces the Phenotypic Transformation of VSMCs by Inhibiting Macrophage Activation in vitro

We evaluated the effects of metformin on macrophage activation in vitro. The transwell assay revealed that metformin administration reduced the number of migrated cells (97.4 ± 20.5 vs 23.2 ± 7.9 in the Ctrl group; Figure 7A and B). To further confirm the hypothesis that metformin inhibits the phenotypic transformation of VSMCs by regulating macrophage activation, we used a co-culture system (Figure 7C), which demonstrated that the pro-inflammatory factors, including iNOS, IL-6, TNF-α, and IL-12A, were downregulated in the culture supernatant of macrophages after metformin administration (Figure 7D–G). Furthermore, metformin treatment resulted in increased levels of SM22α (Figure 7H and I). ELISA results demonstrated that metformin treatment

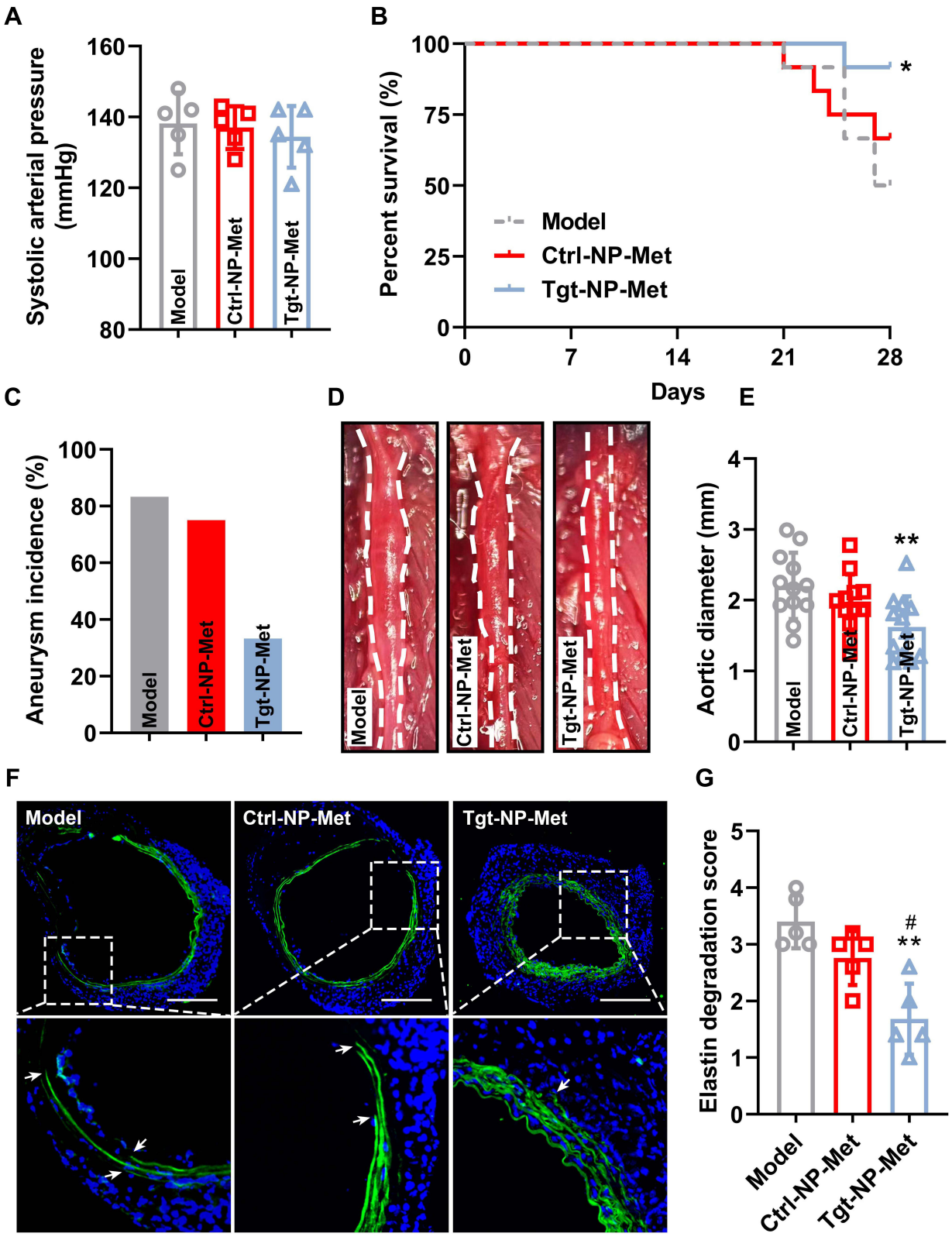

Figure 4 Tgt-NP-Met treatment prevents AAA progression. (**A**) Arterial pressure measurement (n = 5 per group). (**B**) Survival rate curve (n = 12 per group). (**C**) Quantification of the aneurysm incidence in each group (n = 12 per group). (**D**) Representative image of the sacrificed aortas. (**E**) Quantification of the aortic diameter (n = 12 per group). (**F**) Elastin degradation detected using IF staining. Arrowheads indicate elastin rupture. (**G**) Quantification of the elastin degradation score (n = 12 per group). Significance was evaluated using one-way ANOVA with the post-hoc Bonferroni test (**A, E** and **G**) and Log rank test (**B**). *$P < 0.05$, **$P < 0.01$. vs Model; #$P < 0.05$. vs Ctrl-NP-Met.

Abbreviations: AAA, abdominal aortic aneurysm; ANOVA, analysis of variance; Ctrl, control; IF, immunofluorescence; Met, metformin; NPs, nanoparticles.

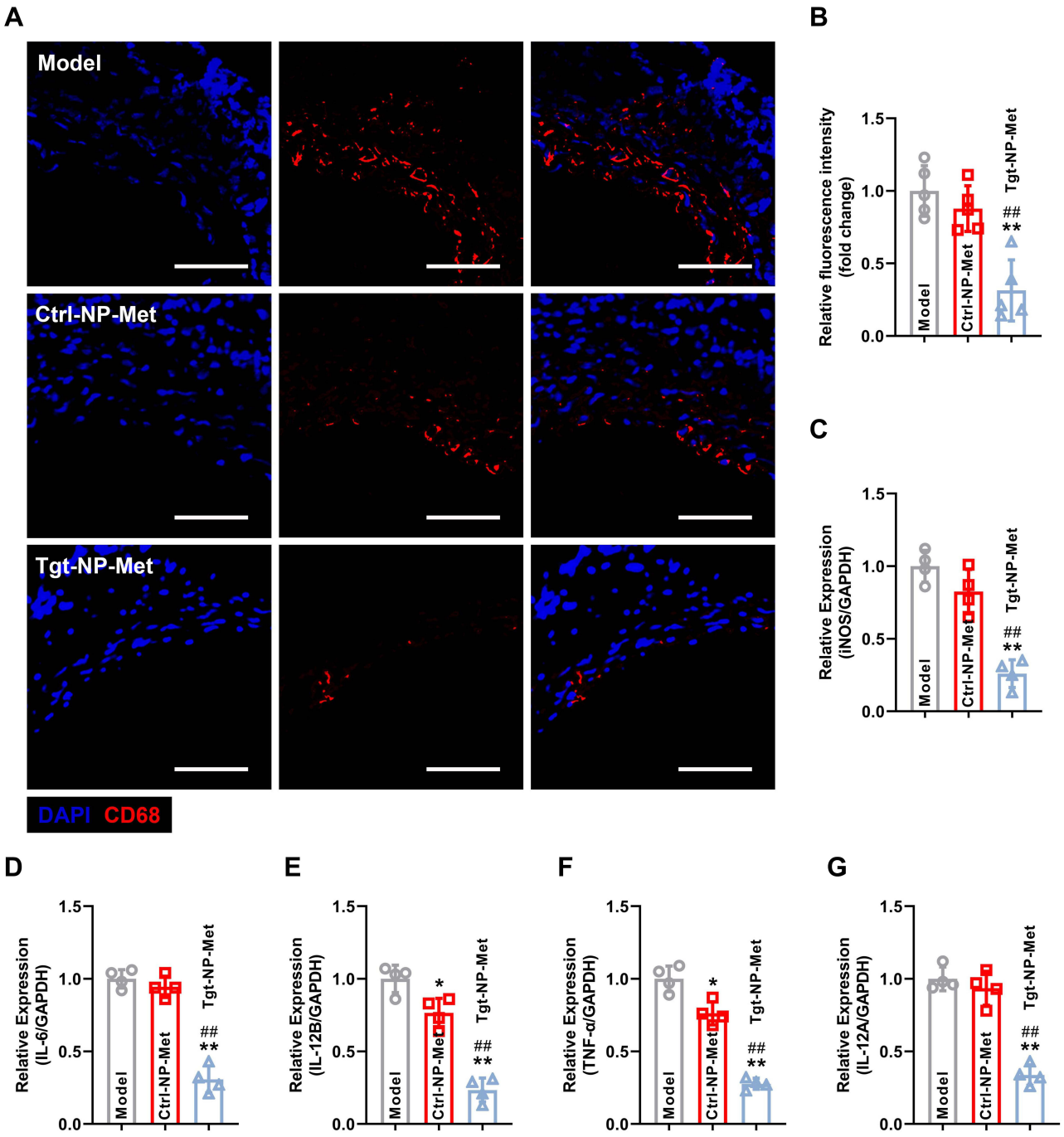

Figure 5 Tgt-NP-Met treatment alleviates macrophage infiltration and M1 polarization in AAAs. (**A**) IF staining of sections of the AAA tissues for CD68 expression (macrophage indicator). Scale bar = 50 μm. (**B**) Quantification of the CD68 fluorescence intensity (n = 5 per group). (**C**–**G**) M1 polarization-related markers, including iNOS (**C**), IL-6 (**D**), TNF-α (**E**), IL-12A (**F**), and IL-12B (**G**), quantified using ELISA. n = 4–5 per group. Significance was evaluated using one-way ANOVA with the post-hoc Bonferroni test. $^{*}P < 0.05$, $^{**}P < 0.01$. vs Model; $^{\#\#}P < 0.01$. vs Ctrl-NP-Met.

Abbreviations: AAA, abdominal aortic aneurysm; ANOVA, analysis of variance; ELISA, enzyme-linked immunosorbent assay; IF, immunofluorescence; Met, metformin; Tgt-NP, targeted nanoparticle.

preserved the contractile phenotypic proteins, including α-SMA, SM22α, Myocd, and Cnn1, which were negatively regulated by LPS (Figure 7J–M). These results indicate that metformin inhibits the phenotypic transformation of VSMCs by regulating macrophage activation.

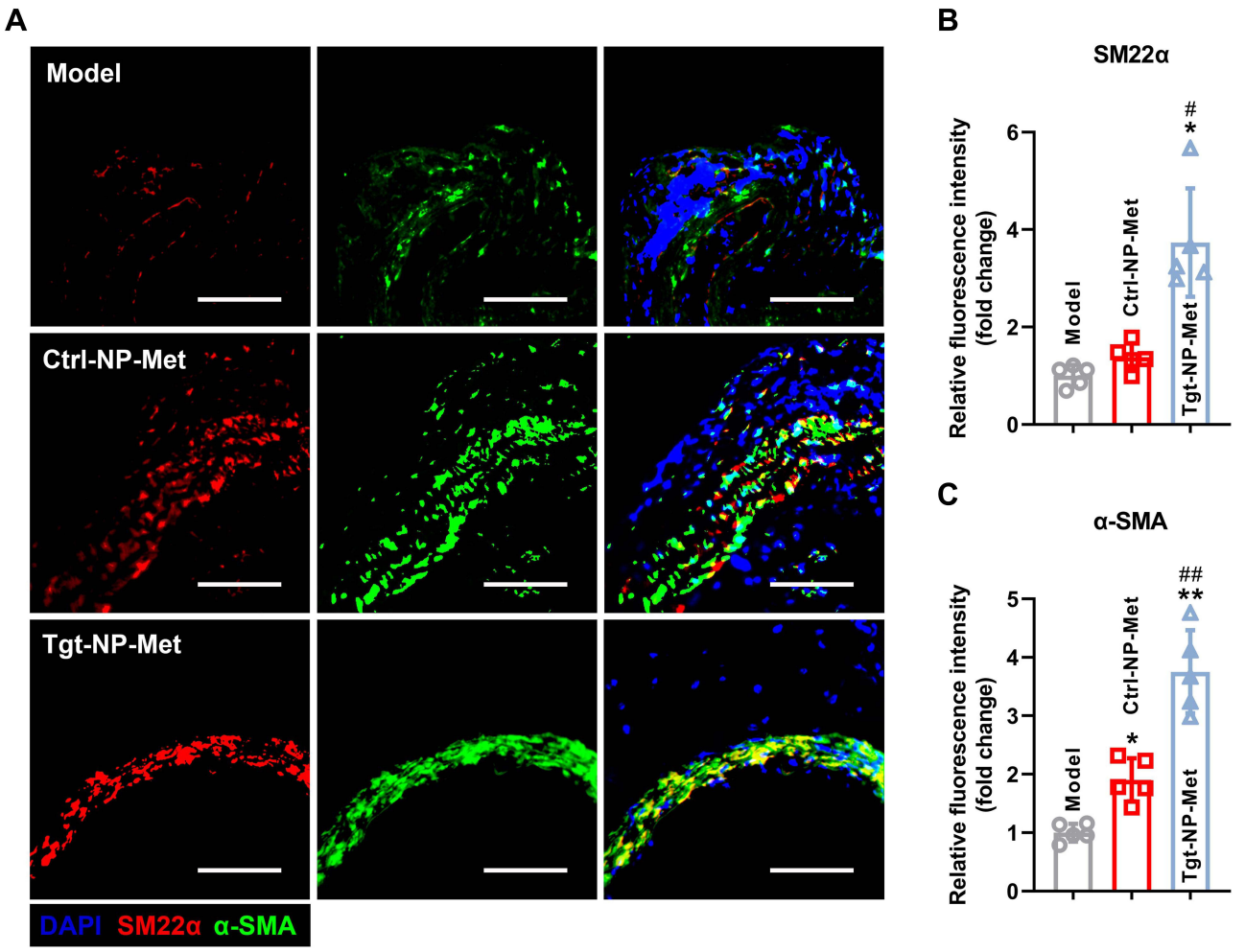

Figure 6 Tgt-NP-Met treatment prevents the phenotypic switch of VSMCs in AAAs. (**A**) IF staining of sections of the AAA tissues for SM22α (contractile phenotype marker; red) and α-SMA (contractile phenotype marker; green) expression. Scale bar = 50 μm. (**B** and **C**) Quantification of the SM22α (**B**) and α-SMA (**C**) fluorescence intensity. N = 5 per group. Significance was evaluated using one-way ANOVA with the post-hoc Bonferroni test. $^{*}P < 0.05$, $^{**}P < 0.01$. vs Model; $^{\#}P < 0.05$, $^{\#\#}P < 0.01$. vs Ctrl-NP-Met.

Abbreviations: AAA, abdominal aortic aneurysm; ANOVA, analysis of variance; Ctrl, control; IF, immunofluorescence; Met, metformin; NP, nanoparticle; VSMCs, vascular smooth muscle cells.

Discussion

AAA causes enormous health and economic burdens globally, and great attempts have been made to manage this life-threatening disease.[1,2] In this study, we designed an AAA-targeted delivery nanoplatform for metformin. After tail vein injection, Tgt-NP-Met adhered to AAA tissues and released metformin sustainably; our major findings are as follows: (i) The netrin-1-responsive AAA-targeted PLGA-PEG nanoplatform can efficiently deliver metformin into AAA tissues; (ii) Tgt-NP-Met administration prevents aneurysm development and attenuates vascular remodeling in an Ang II–induced AAA mouse model; and (iii) metformin inhibits the transformation of VSMCs from a contractile phenotype to a synthetic phenotype by regulating macrophage infiltration and activation in AAA. These findings provide evidence that targeting nanoplatform-based metformin is a novel and efficient strategy for AAA therapy.

Multiple drugs exhibit therapeutic potential for diseases at the cellular level.[1] However, these drugs have limited clinical application owing to the lack of effective specific tissue-targeting delivery vehicles. Furthermore, thus far, few efficient targeted delivery nanoplatforms for AAA tissues have been developed. Targeting ligand-modified polymeric NPs holds great promise in overcoming this dilemma. Aptamers, peptides, and mAbs are the most commonly used ligands for this purpose.[17] Aptamers are a small segment of nucleic acids that can bind to specific ligands based on their three-dimensional structures. Although aptamers have advantages, including ease of synthesis, a wide range of targets,

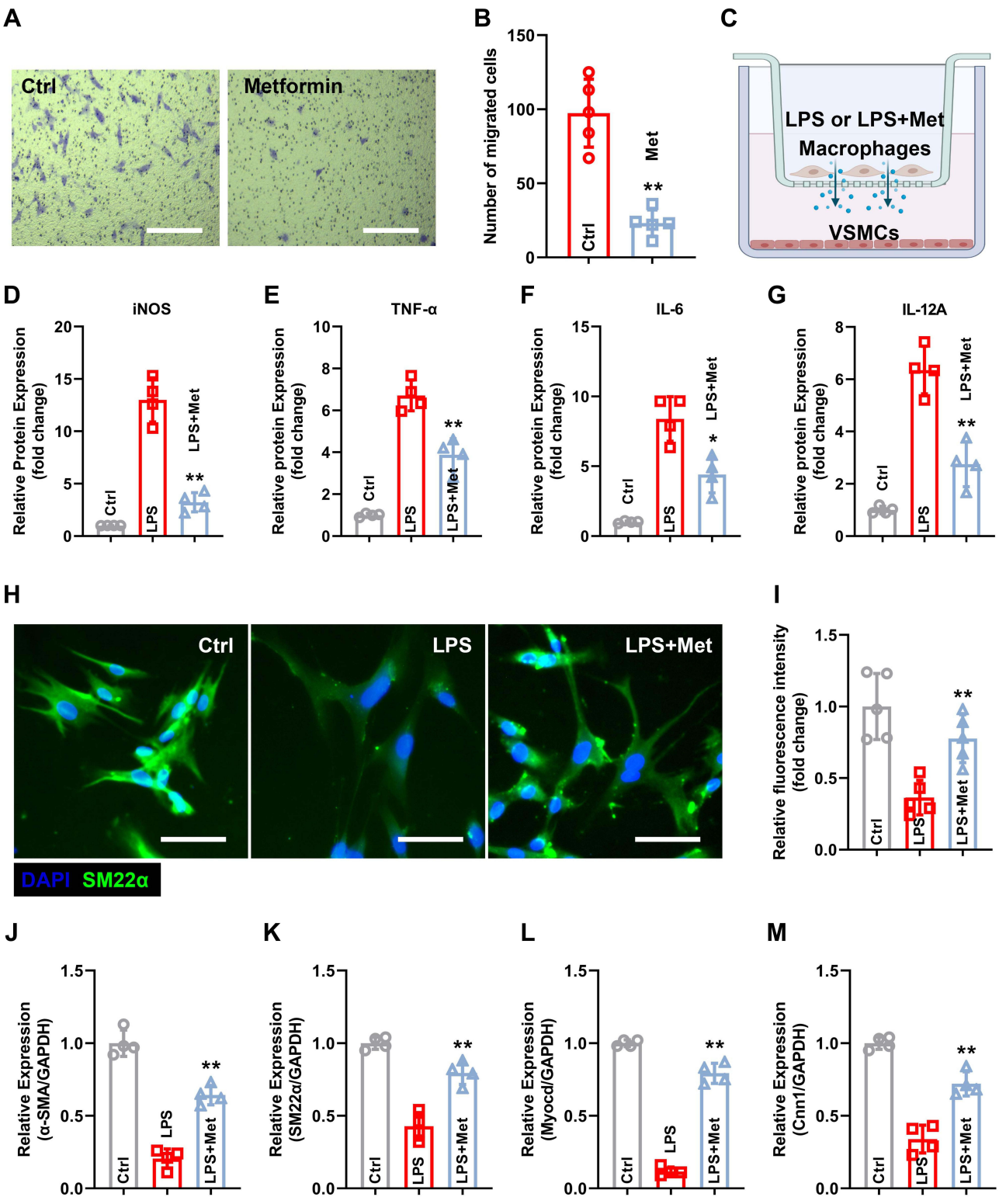

Figure 7 Metformin inhibits macrophage M1 polarization and subsequently alleviates the phenotypic switch of VSMCs in vitro. (**A**) Macrophage migration ability was evaluated using transwell assay. Scale bar = 50 μm. (**B**) Quantification of the number of migrated cells. (**C**) Schematic diagram of the co-culture system. (**D**–**G**) M1 polarization-related markers, including iNOS (**D**), IL-6 (**E**), TNF-α (**F**), and IL-12A (**G**), were quantified using ELISA. (**H**) IF staining of VSMCs for SM22α expression. Scale bar = 50 μm. (**I**) Quantification of the SM22α fluorescence intensity. (**J**–**M**) Contractile phenotype markers, including α-SMA (**J**), SM22α (**K**), Myocd (**L**), and Cnn1 (**M**), were quantified using ELISA. n = 4–5 per group. Significance was evaluated using Student's *t*-test (**B**) and one-way ANOVA with the post-hoc Bonferroni test (**D**–**G** and **I**–**M**). **P* < 0.05, ***P* < 0.01.

Abbreviations: AAA, abdominal aortic aneurysm; ANOVA, analysis of variance; ELISA, enzyme-linked immunosorbent assay; IF, immunofluorescence; VSMCs, vascular smooth muscle cells.

https://doi.org/10.2147/IJN.S400993 DovePress

and low immunogenicity, and exhibit excellent performance in vitro, their clinical application still faces great challenges. For instance, non-specific binding proteins in the human body reduce the targeting efficiency of aptamers through competitive binding. In addition, aptamers can be easily degraded in the human circulatory system owing to the presence of nucleases.[18] Peptides are another potential ligand for targeting NPs. Various tissue-specific peptides, including those in the brain, pancreas, kidney, liver, and lung, have been recognized and achieved desirable results in vitro.[19] However, similar to aptamers, targeting peptides also exhibit a lack of stability and low targeting efficiency in in vivo investigations.[20] Therefore, in the present study, we chose mAbs as ligands for PLGA-PEG-targeted modification. Our in vivo results demonstrated that the binding of netrin-1 mAbs significantly enhanced the AAA-targeting capacity of PLGA-PEG NPs. Both bioluminescence and IF staining provided solid evidence for this result. These findings indicate that mAbs are the most effective targeting modification ligands in vivo.

Recent epidemiological investigations have reported that metformin could reduce the incidence of aortic aneurysms and further inhibit the expansion of small AAAs (diameter ranging from 30 mm to 50 mm).[8] These conclusions are consistent with the experimental results of this study. However, the crucial role of metformin in vascular remodeling remains unclear. Macrophage recruitment and M1 polarization, which contribute to pro-inflammatory cytokine production, are early events in AAA progression.[15] Thus, blocking macrophage aggregation and M1 polarization may potentially reverse the vascular remodeling of AAA. Interestingly, our results illustrate that Tgt-NP-Met administration reduces macrophage infiltration and M1 polarization, as evidenced by the downregulation of M1 polarization-related proteins, including iNOS, IL-6, TNF-α, IL-12A, and IL-12B, in the AAA tissues. These findings suggest the therapeutic potential of metformin in preventing small AAA progression via direct modulation of macrophage polarization.

The major pathological process of AAA is characterized by inflammatory cell infiltration, extracellular matrix (ECM) degradation, and VSMC transformation.[21] Under physiological conditions, VSMCs exhibit a contractile phenotype that regulates blood flow and pressure, whereas under AAA conditions, they transform to a synthetic phenotype that secretes matrix metalloproteinase-2 (MMP-2), MMP-9, and cathepsins, which trigger elastin degradation.[22,23] ECM degradation is attributed to vascular remodeling and aortic wall weakening. Although the phenotypic switch of VSMCs plays a key role in the occurrence of AAA, the specific mechanism underlying this phenotypic transformation of VSMCs in AAA remains unclear. Our in vitro experiment results demonstrated that the contractile phenotype-related markers of VSMCs, including α-SMA, SM22α, Myocd, and Cnn1, were significantly downregulated when co-cultured with LPS-activated macrophages. Moreover, metformin administration attenuated the M1 macrophage-induced process. In addition, some previous studies reveal that macrophage not only regulates phenotypic switch of VSMCs, but also determine the fate of vascular endothelial cells (ECs) in AAA. More detailed studies are needed in the future to reveal the deeper relationship of macrophage, VSMCs and ECs in time sequence and space sequence during AAA formation.[23,24] Therefore, the observed effects of metformin on the phenotypic transformation of VSMCs in our experiments may be mediated, at least in part, via regulation of macrophage activity.

Limitation

In this study, we used mice to establish the AAA model. However, the differences in hemodynamic and electrophysiological properties between mice and humans make it impossible to directly translate the research data from rodent models to humans. Therefore, future studies should establish preclinical models, such as swine and non-human primate models, to evaluate the efficacy and safety of Tgt-NP-Met administration for AAA management.

Conclusion

This study revealed that a netrin-1-responsive AAA-targeted nanoplatform can efficiently deliver metformin into AAA tissues. Metformin exerts a therapeutic effect on AAA by inhibiting the phenotypic switch of VSMCs that is triggered by macrophage activation.

Acknowledgment

This work was supported by the National Natural Science Foundation of China (No. 81970397); Science and Technology Program of Xiamen (3502Z20194009).

Disclosure

The authors declare that they have no competing interests in this work.

References

1. Golledge J. Abdominal aortic aneurysm: update on pathogenesis and medical treatments. *Nat Rev Cardiol*. 2019;16(4):225–242. doi:10.1038/s41569-018-0114-9
2. Chaikof EL, Dalman RL, Eskandari MK, et al. The society for vascular surgery practice guidelines on the care of patients with an abdominal aortic aneurysm. *J Vasc Surg*. 2018;67(1):2–77 e2. doi:10.1016/j.jvs.2017.10.044
3. Sakalihasan N, Michel JB, Katsargyris A, et al. Abdominal aortic aneurysms. *Nat Rev Dis Primers*. 2018;4(1):34. doi:10.1038/s41572-018-0030-7
4. Flory J, Lipska K. Metformin in 2019. *JAMA*. 2019;321(19):1926–1927. doi:10.1001/jama.2019.3805
5. Madiraju AK, Qiu Y, Perry RJ, et al. Metformin inhibits gluconeogenesis via a redox-dependent mechanism in vivo. *Nat Med*. 2018;24(9):1384–1394. doi:10.1038/s41591-018-0125-4
6. Triggle CR, Mohammed I, Bshesh K, et al. Metformin: is it a drug for all reasons and diseases? *Metabolism*. 2022;133:155223. doi:10.1016/j.metabol.2022.155223
7. Raffort J, Hassen-Khodja R, Jean-Baptiste E, Lareyre F. Relationship between metformin and abdominal aortic aneurysm. *J Vasc Surg*. 2020;71(3):1056–1062. doi:10.1016/j.jvs.2019.08.270
8. Wanhainen A, Unosson J, Mani K, Gottsater A, Investigators MT. The metformin for abdominal aortic aneurysm growth inhibition (MAAAGI) trial. *Eur J Vasc Endovasc Surg*. 2021;61(4):710–711. doi:10.1016/j.ejvs.2020.11.048
9. Graham GG, Punt J, Arora M, et al. Clinical pharmacokinetics of metformin. *Clin Pharmacokinet*. 2011;50(2):81–98. doi:10.2165/11534750-000000000-00000
10. Soukas AA, Hao H, Wu L. Metformin as anti-aging therapy: is it for everyone? *Trends Endocrinol Metab*. 2019;30(10):745–755. doi:10.1016/j.tem.2019.07.015
11. Jin K, Luo Z, Zhang B, Pang Z. Biomimetic nanoparticles for inflammation targeting. *Acta Pharm Sin B*. 2018;8(1):23–33. doi:10.1016/j.apsb.2017.12.002
12. Duan H, Liu Y, Gao Z, Huang W. Recent advances in drug delivery systems for targeting cancer stem cells. *Acta Pharm Sin B*. 2021;11(1):55–70. doi:10.1016/j.apsb.2020.09.016
13. Chen X, Lisi F, Bakthavathsalam P, et al. Impact of the Coverage of Aptamers on a Nanoparticle on the Binding Equilibrium and Kinetics between Aptamer and Protein. *ACS Sens*. 2021;6(2):538–545. doi:10.1021/acssensors.0c02212
14. Chen Q, Xu L, Liang C, Wang C, Peng R, Liu Z. Photothermal therapy with immune-adjuvant nanoparticles together with checkpoint blockade for effective cancer immunotherapy. *Nat Commun*. 2016;7:13193. doi:10.1038/ncomms13193
15. Hadi T, Boytard L, Silvestro M, et al. Macrophage-derived netrin-1 promotes abdominal aortic aneurysm formation by activating MMP3 in vascular smooth muscle cells. *Nat Commun*. 2018;9(1):5022. doi:10.1038/s41467-018-07495-1
16. Shrestha N, Xu Y, Prevost JRC, et al. Impact of PEGylation on an antibody-loaded nanoparticle-based drug delivery system for the treatment of inflammatory bowel disease. *Acta Biomater*. 2022;140:561–572. doi:10.1016/j.actbio.2021.12.015
17. Yan J, Gao T, Lu Z, Yin J, Zhang Y, Pei R. Aptamer-targeted photodynamic platforms for tumor therapy. *ACS Appl Mater Interfaces*. 2021;13(24):27749–27773. doi:10.1021/acsami.1c06818
18. Vazquez-Gonzalez M, Willner I. Aptamer-functionalized micro- and nanocarriers for controlled release. *ACS Appl Mater Interfaces*. 2021;13(8):9520–9541. doi:10.1021/acsami.0c17121
19. Ding B, Sheng J, Zheng P, et al. Biodegradable upconversion nanoparticles induce pyroptosis for cancer immunotherapy. *Nano Lett*. 2021;21(19):8281–8289. doi:10.1021/acs.nanolett.1c02790
20. Galloway JM, Bray HEV, Shoemark DK, et al. De novo designed peptide and protein hairpins self-assemble into sheets and nanoparticles. *Small*. 2021;17(10):e2100472. doi:10.1002/smll.202100472
21. Lu H, Du W, Ren L, et al. Vascular smooth muscle cells in aortic aneurysm: from genetics to mechanisms. *J Am Heart Assoc*. 2021;10(24):e023601. doi:10.1161/JAHA.121.023601
22. Pan L, Bai P, Weng X, et al. Legumain is an endogenous modulator of integrin alphavbeta3 triggering vascular degeneration, dissection, and rupture. *Circulation*. 2022;145(9):659–674. doi:10.1161/CIRCULATIONAHA.121.056640
23. Li J, Li W, Zou D, et al. Comparison of conjugating chondroitin sulfate A and B on amine-rich surface: for deeper understanding on directing cardiovascular cells fate. *Compos B Eng*. 2022;228:109430. doi:10.1016/j.compositesb.2021.109430
24. Filiberto AC, Spinosa MD, Elder CT, et al. Endothelial pannexin-1 channels modulate macrophage and smooth muscle cell activation in abdominal aortic aneurysm formation. *Nat Commun*. 2022;13(1):1521. doi:10.1038/s41467-022-29233-4